

Raman characterization of electronic properties of self-assembled GaN nanorods grown by plasma-assisted molecular-beam epitaxy

D. Wang, C. -C. Tin, J. R. Williams, M. Park, Y. S. Park, C. M. Park, T. W. Kang, and W. -C. Yang

Citation: [Applied Physics Letters](#) **87**, 242105 (2005); doi: 10.1063/1.2146066

View online: <http://dx.doi.org/10.1063/1.2146066>

View Table of Contents: <http://scitation.aip.org/content/aip/journal/apl/87/24?ver=pdfcov>

Published by the [AIP Publishing](#)

Articles you may be interested in

[Germanium doping of self-assembled GaN nanowires grown by plasma-assisted molecular beam epitaxy](#)
J. Appl. Phys. **114**, 103505 (2013); 10.1063/1.4820264

[In situ study of self-assembled GaN nanowires nucleation on Si\(111\) by plasma-assisted molecular beam epitaxy](#)
Appl. Phys. Lett. **100**, 212107 (2012); 10.1063/1.4721521

[Raman scattering of phonon-plasmon coupled modes in self-assembled GaN nanowires](#)
J. Appl. Phys. **105**, 123707 (2009); 10.1063/1.3148862

[Nucleation and growth of GaN nanorods on Si \(111\) surfaces by plasma-assisted molecular beam epitaxy - The influence of Si- and Mg-doping](#)
J. Appl. Phys. **104**, 034309 (2008); 10.1063/1.2953087

[Self-assembled vertical GaN nanorods grown by molecular-beam epitaxy](#)
Appl. Phys. Lett. **82**, 1601 (2003); 10.1063/1.1558216

The image shows the cover of the journal Applied Physics Reviews. It features a blue and orange color scheme with a molecular structure graphic. The text 'AIP Applied Physics Reviews' is at the top. Below it, there is a diagram of a device structure and a graph. The text 'april-apr 2015' is at the bottom left.

NEW Special Topic Sections

NOW ONLINE
Lithium Niobate Properties and Applications:
Reviews of Emerging Trends

AIP Applied Physics Reviews

Raman characterization of electronic properties of self-assembled GaN nanorods grown by plasma-assisted molecular-beam epitaxy

D. Wang, C. -C. Tin, J. R. Williams, and M. Park^{a)}

Laboratory for Nanophotonics and Department of Physics, Auburn University, Auburn, Alabama 36849

Y. S. Park, C. M. Park, T. W. Kang, and W. -C. Yang

Quantum Functional Semiconductor Research Center and Department of Physics, Dongguk University, Seoul 100-715, Korea

(Received 20 June 2005; accepted 21 October 2005; published online 8 December 2005)

We have investigated the Raman scattering of the aligned gallium nitride (GaN) nanorods grown by plasma-assisted molecular-beam epitaxy. It was determined by Raman spectroscopy that the GaN nanorods are relatively strain free. The free carrier concentration, as well as electron mobility of the GaN nanorods, was obtained by the line shape analysis of the coupled A_1 longitudinal-optical (LO) phonon-plasmon mode. The electron concentration and mobility of electron obtained from line shape analysis are $3.3 \times 10^{17} \text{ cm}^{-3}$ and $140 \text{ cm}^2 \text{ V s}$, respectively. The local temperature of the nanorod sample was estimated based on the ratio of Stokes to anti-Stokes Raman peak intensity. Since the position of the LO phonon peak was found to be dependent on both the temperature and the LO phonon-plasmon coupling, it is crucial to consider the temperature effect in determining the frequency of the uncoupled LO phonon mode for the line shape analysis. The frequency of the $A_1(\text{LO})$ mode of an undoped bulk GaN was used as a reference to determine the frequency of the uncoupled $A_1(\text{LO})$ phonon mode of the GaN nanorods. © 2005 American Institute of Physics.

[DOI: 10.1063/1.2146066]

In polar semiconductors, the longitudinal-optical (LO) phonons couple strongly with plasmon through the macroscopic electric field.¹ The coupling between the plasmon and the LO phonon produce two coupled LO phonon-plasmon (LPP) modes, the $\omega_+(\text{LPP}^+)$ and the $\omega_-(\text{LPP}^-)$ (high- and low-frequency modes, respectively).² The coupling is through the macroscopic electric fields of these excitations. The high-frequency LPP^+ mode behaves like an LO phonon at low carrier densities. The frequency of the LPP^+ mode increases with carrier concentration, and eventually corresponds to that of the plasmon. Such a mode was proposed by Varga,³ and first observed in GaAs by Mooradian and Wright.²

When plasmon damping is substantial, the coupling will be displayed as a shift of LO phonon mode. In GaN, it was observed that the LO phonon modes couple with the plasmon mode. Compared with the uncoupled LO phonon peak, the LPP mode is shifted to higher frequency and asymmetrically broadened with increasing free-carrier concentration. The LPP mode also depends on the LO phonon damping as well as the plasmon damping constant, and this fact can be exploited to extract the charge concentration and carrier mobility from Raman spectra. Raman spectroscopy has been used to deduce the electron concentration and electron mobility in thin films and bulk GaN by many researchers.^{4–11} However, this method has not been applied to the analysis of electronic properties of nanowires, where it will be difficult to employ electronic approach due to the difficulty of contact preparation. Therefore, in the present work, we have demonstrated that electronic properties of nanowires can be obtained via Raman spectroscopy. We also considered the effect of local laser heating on the Raman peak shift since there is a sub-

stantial increase in the temperature of the nanowire during Raman measurements due to the lack of heat dissipation.

In the present investigation, *c*-axis aligned GaN nanorods were grown on a Si (111) substrate using a radio-frequency (rf) plasma-assisted molecular-beam epitaxy (PAMBE). The Si substrate was degreased and then etched with HF and followed by thermal treatment at 900 °C for 30 min. The cleaned substrate showed a reconstructed (7×7) surface with measurement of reflection high-energy electron diffraction. All growth procedures of GaN nanorods were carried out under N-rich conditions. The rf-plasma power was kept constant at 350 W during the growth. The growth rate was $1.5 \mu\text{m/h}$. The details of the sample preparation steps can be found elsewhere.¹² The morphology of the sample was characterized using a high-resolution scanning electron microscopy (HR-SEM) (see Fig. 1). Micro-Raman spectroscopy was carried out using a backscattering geometry. The wavelength of 441.6 nm line of the Kimmon Electric's HeCd laser was used as an excitation. The polarization states of the incident and the scattered beam were not analyzed. The laser beam with a nominal power of 80 mW was focused onto a spot with $\sim 5 \mu\text{m}$ in diameter. The Jobin-Yvon's spectrometer with a thermoelectrically cooled charge coupled device detector was used to collect the Stokes' and anti-Stokes' Raman spectra.

According to group theory, $A_1(z) + 2B_1 + E_1(x, y) + 2E_2$ optical modes are predicted at the Γ point of the Brillouin zone of hexagonal GaN.¹³ The two E_2 modes are Raman active, the A_1 and E_1 modes are both Raman and infrared active, and the two B_1 modes are optically silent. Since the A_1 and E_1 modes are polar, they split into LO and transverse-optical (TO) components. According to the Raman selection rules, only the $E_2^{(1)}$, $E_2^{(2)}$, and $A_1(\text{LO})$ modes can be observed with the $z(-,-)z$ scattering geometry of this experiment.

^{a)}Electronic mail: park@physics.auburn.edu

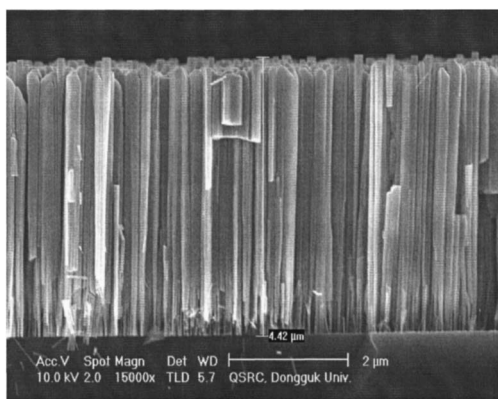


FIG. 1. A cross-sectional HR-SEM micrograph of the GaN nanorods grown on a Si(111) substrate.

Figure 2 shows the Stokes and anti-Stokes Raman spectrum for the GaN nanorods, the Raman spectrum of a single-crystal bulk GaN sample (Kyma Technologies, Inc.) was also collected for comparison. The electron concentration of the bulk GaN obtained using *C-V* measurement is $<10^{16} \text{ cm}^{-3}$. It was also assumed that the bulk GaN is strain free. In addition to the theoretically allowed modes, $A_1(\text{TO})$ and $E_1(\text{TO})$ are also present in the Raman spectrum of nanorods, which is possibly caused by the imperfect alignment of the nanorods and the finite collection angle of the microscope objective.

Upon illumination by focused laser beam, the local temperature of the sample can reach several hundred degrees Celsius, possibly causing downshift and broadening of the Raman peak. This heating effect is especially pronounced in micro or nanostructured materials due to their reduced thermal conductivities.¹⁴ Without taking the thermal effect into account, the experimental results can be misleading.¹⁴ There-

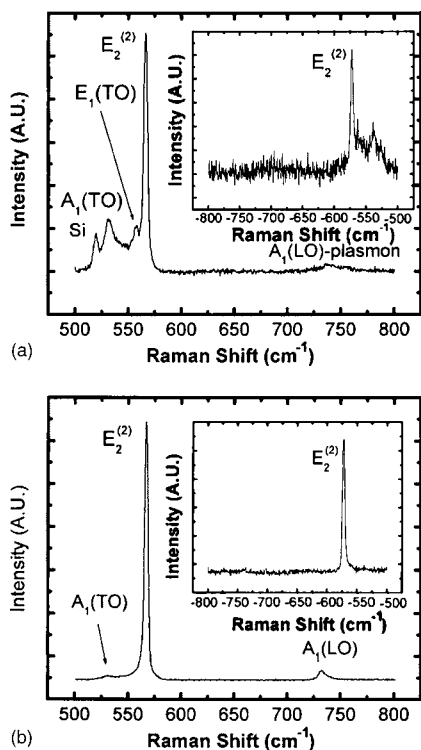


FIG. 2. Raman spectrum of the GaN nanorod (a) and bulk GaN (b). The insets show the anti-Stokes part of the spectrum.

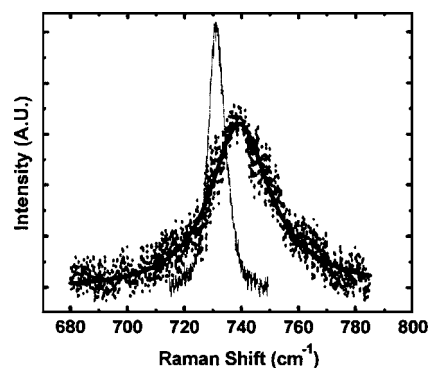


FIG. 3. Raman spectrum of the LPP coupled mode for GaN nanorod (dotted line) and bulk GaN (dashed line). The thick solid lines are the fitting curves for nanorods by line shape analysis. The shift and broadening of the LLP mode are obvious with respect to the uncoupled $A_1(\text{LO})$ mode of the bulk GaN.

fore, the integrated intensity of E_2 phonon peaks for both Stokes (I_S) and anti-Stokes (I_{AS}) were obtained to estimate the local temperature of the samples. The local temperature was calculated using the following relationship:¹⁵

$$I_S/I_{AS} \propto \exp(\hbar\omega_{E_2}/k_B T), \quad (1)$$

where ω_{E_2} is the E_2 phonon mode frequency. The estimated temperatures are 505 K and 460 K for the GaN nanorods and the single-crystal bulk GaN, respectively.

The temperature dependence of Raman scattering in GaN has been studied.^{16,17} Based on Li *et al.*'s work,¹⁵ we have obtained the Raman peak positions using the estimated temperature (hereafter to be referred to as "temperature-calibrated" peak position). It was found that the temperature-calibrated E_2 mode frequency for the single-crystal GaN is the same as what was measured by Raman scattering. The temperature-calibrated $A_1(\text{TO})$ and $E_1(\text{TO})$ mode frequencies of the GaN nanorods are also in excellent agreement with the observed experimental values. This can be an alternative way to verify the estimated temperatures. The measured E_2 mode frequency of the nanorods is very close to the temperature-calibrated value. Therefore, it can be concluded that our nanorods are relatively strain-free.

Due to both the scattering geometry and the aligned nature of the nanorods used in this work, we can expect that the observed LO peak is $A_1(\text{LO})$ mode. Therefore, no intermixing between the $E_1(\text{LO})$ and $A_1(\text{LO})$ mode can be expected. In order to determine the exact position of the uncoupled $A_1(\text{LO})$ mode, it is important to prevent $A_1(\text{LO})$ mode from being coupled with $E_1(\text{LO})$ mode since the intermixing of the two LO phonon modes leads to the change of the LO mode peak position.¹⁸ Since $A_1(\text{LO})$ phonons polarize along the c axis of the wurtzite unit cell, the plasmon oscillations coupled to it also polarize in that direction. Subsequently, the physical parameters involved in the process such as the damping constants are those defined along the c axis assuming the anisotropy of the wurzite crystal.

The intensity of the LPP mode is given by¹⁹

$$I(\omega) = \text{Const.} \cdot A(\omega) \cdot \text{Im}[-\epsilon(\omega)^{-1}], \quad (2)$$

where the $A(\omega)$ corrects for the deformation-potential and electro-optic mechanism.¹⁸ By fitting the Raman spectrum of the LPP mode with the functional form given in Eq. (2), the plasmon frequency ω_p , plasmon damping constant γ , and

TABLE I. Parameters used in the line shape analysis, and the fitting results for the plasma frequency, phonon damping constant, and plasmon damping constant (all in cm^{-1}).

	$\omega_{\text{TO}}^{\text{a}}$	$\omega_{\text{LO}}^{\text{b}}$	$\varepsilon_{\infty\perp}^{\text{c}}$	ω_p	Γ	γ	$n_e(10^{17} \text{ cm}^{-3})$	$\mu(\text{cm}^2/\text{V s})$
Nanorod	531.7	731.2	5.35	169.4	18.4	347	3.3	140

^aObtained by fitting the Raman spectrum with Lorentzian function.^bCalculated by considering the temperature effect. Obtained using the uncoupled $A_1(\text{LO})$ peak position of the bulk GaN.^cSee Ref. 19.

phonon damping constant Γ can be extracted. The free-carrier concentration n_e and mobility μ can then be derived from the plasmon frequency and plasmon damping constant as

$$\omega_p = \sqrt{\frac{4\pi n e^2}{\varepsilon_{\infty} m^*}}, \quad (3)$$

$$\gamma = \frac{e}{m^* \mu}, \quad (4)$$

where m^* is the effective mass of the free carrier, and $m^* = 0.22m_e$ in the case for GaN.²⁰

Satisfactory fitting results were obtained in the region of LPP mode for GaN nanorods and single-crystal bulk GaN, as shown in Fig. 3. The fitting parameters and results are summarized in Table I. The electron concentration and mobility of electron obtained from line shape analysis are $3.3 \times 10^{17} \text{ cm}^{-3}$ and $140 \text{ cm}^2/\text{V s}$, respectively. The frequency for $A_1(\text{TO})$ mode, ω_{TO} , can be readily obtained from the Raman spectrum. However, care must be taken to specify the frequency for the uncoupled $A_1(\text{LO})$ mode: ω_{LO} . Instead of blindly using 734 cm^{-1} which has been widely adopted as the frequency for the uncoupled $A_1(\text{LO})$,²¹ the temperature-calibrated $A_1(\text{LO})$ frequency should be used as ω_{LO} . Since the electron concentration of the undoped bulk GaN is $<10^{16} \text{ cm}^{-3}$, the $A_1(\text{LO})$ mode in the undoped bulk GaN is not shifted due to the LO phonon-plasmon coupling.²² Therefore, we can use the value as the frequency of the uncoupled $A_1(\text{LO})$ mode at $T=460 \text{ K}$. We then downshifted it by 1.3 cm^{-1} to obtain the frequency of the uncoupled $A_1(\text{LO})$ mode at $T=505 \text{ K}$ (the temperature of the nanorods), thus $\omega_{\text{LO}}=731.2 \text{ cm}^{-1}$ is the frequency of the uncoupled $A_1(\text{LO})$ mode used in the curve fitting. This precaution is further justified by the fact that the frequency of the $A_1(\text{LO})$ mode of the undoped bulk GaN is at 732.5 cm^{-1} which is downshifted compared with 734 cm^{-1} due to the elevated temperature.

In summary, we have investigated the Raman scattering of the aligned GaN nanorods grown by PAMBE. It was determined by Raman spectroscopy that the GaN nanorods are relatively strain free. The free-carrier concentration, as well as electron mobility of the GaN nanorods, was obtained by the line shape analysis of the coupled $A_1(\text{LO})$ phonon-plasmon mode. The electron concentration and mobility of electron obtained from line shape analysis are $3.3 \times 10^{17} \text{ cm}^{-3}$ and $140 \text{ cm}^2/\text{V s}$, respectively. The local temperature of the nanorod sample was estimated based on the ratio of Stokes to anti-Stokes Raman peak intensity. Since the position of the LO phonon peak was found to be dependent on both the temperature and the LO phonon-

plasmon coupling, it is crucial to consider temperature effect in determining the frequency of the uncoupled LO phonon mode for the line shape analysis. The frequency of $A_1(\text{LO})$ mode of an undoped bulk GaN was used as a reference to determine the frequency of the uncoupled $A_1(\text{LO})$ phonon mode of the GaN nanorods.

One of the authors (M.P.) would like to thank Mark Williams at Kyma Technologies, Inc., for supplying bulk GaN for this study. The authors also acknowledges the support from the Quantum Functional Semiconductor Research Center at Dongguk University.

¹M. V. Klein, in *Light Scattering in Solids*, edited by M. Cardona (Springer, Berlin, 1975).

²A. Mooradian and G. B. Wright, *Phys. Rev. Lett.* **16**, 999 (1966).

³B. B. Varga, *Phys. Rev. A* **137**, 1896 (1965).

⁴T. Kozawa, T. Kachi, H. Kano, Y. Taga, M. Hashimoto, N. Koide, and K. Manabe, *J. Appl. Phys.* **75**, 1098 (1994).

⁵P. Perlin, J. Camassel, W. Knap, T. Taliercio, J. C. Chervin, T. Suski, I. Grzegory, and S. Porowski, *Appl. Phys. Lett.* **67**, 2524 (1995).

⁶H. Harima, H. Sakashita, and S. Nakashima, *Mater. Sci. Forum* **264**, 1363 (1998).

⁷N. Wieser, M. Klose, F. Scholz, and J. Off, *Mater. Sci. Forum* **264**, 1351 (1998).

⁸D. Meister, M. Böhm, M. Topf, W. Kriegseis, W. Burkhardt, I. Dirnstorfer, S. Rösel, B. Farangis, B. K. Meyer, A. Hoffmann, H. Siegle, C. Thomsen, J. Christen, and F. Bertram, *J. Appl. Phys.* **88**, 1811 (2000).

⁹H. Siegle, A. Hoffmann, L. Eckey, C. Thomsen, J. Christen, F. Bertram, D. Schmidt, D. Rudloff, and K. Hiramatsu, *Appl. Phys. Lett.* **71**, 2490 (1997).

¹⁰E. Frayssinet, W. Knap, S. Krukowski, P. Perlin, P. Wisniewski, T. Suski, I. Grzegory, and S. Porowski, *J. Cryst. Growth* **230**, 442 (2001).

¹¹M. Park, J. J. Cuomo, W.-C. Yang, B. J. Rodriguez, R. J. Nemanich, and O. Ambacher, *J. Appl. Phys.* **93**, 9542 (2003).

¹²Y. S. Park, C. M. Park, D. J. Fu, T. W. Kang, and J. E. Oh, *Appl. Phys. Lett.* **85**, 5718 (2004); Y. S. Park, S. H. Lee, J. E. Oh, C. M. Park, and T. W. Kang, *J. Cryst. Growth* (to be published).

¹³W. Hayes and R. Loudon, *Scattering of Light by Crystals* (Wiley, New York, 1978).

¹⁴K. A. Alim, V. A. Fonobeov, and A. A. Balndin, *Appl. Phys. Lett.* **86**, 053103 (2005).

¹⁵M. Balkanski, R. F. Wallis, and E. Haro, *Phys. Rev. B* **28**, 1928 (1983).

¹⁶W. S. Li, Z. X. Shen, Z. C. Feng, and S. J. Chua, *J. Appl. Phys.* **87**, 3332 (2000).

¹⁷M. S. Liu, L. A. Bursill, S. Praver, K. Nugent, Y. Z. Tong, and G. Y. Zhang, *Appl. Phys. Lett.* **74**, 3125 (1999).

¹⁸C. A. Arguello, D. L. Rousseau, and S. P. S. Porto, *Phys. Rev.* **181**, 1351 (1969).

¹⁹G. Irmer, V. V. Toporov, B. H. Bairamov, and J. Monecke, *Phys. Status Solidi B* **119**, 595 (1983).

²⁰K. H. Hellwege, O. Madelung, and A. M. Hellege, *Numerical Data and Functional Relationship in Science and Technology* (Springer, New York, 1987).

²¹F. Demangeot, J. Frandon, M. A. Renucci, C. Meny, O. Briot, and R. L. Aulombard, *J. Appl. Phys.* **82**, 1305 (1997).

²²M. Park, J.-P. Maria, J. J. Cuomo, Y. C. Chang, J. F. Muth, R. M. Kolbas, R. J. Nemanich, E. Carlson, and J. Bumgarner, *Appl. Phys. Lett.* **81**, 1797 (2002).